

Characterization of Ti6Al4V Alloy Produced by Laser-Powder Bed Fusion and Surface Modification Using Nanosecond Laser

Gleicy de Lima Xavier Ribeiro^{a,b,*} , Renato Spacini de Castro^a , Rogério Góes dos Santos^a ,
Aline de Fátima Santos Bugarin^{a,b} , Maysa Terada^a , Gilmar Ferreira Batalha^c ,
Antônio Couto^{b,d} 

^aInstituto Senai de Inovação em Manufatura Avançada e Microfabricação, Rua Bento Branco de Andrade, 379, Santo Amaro, 04757-000, São Paulo, SP, Brasil.

^bInstituto de Pesquisas Energéticas e Nucleares, Av. Lineu Prestes, 2242, 05508-000, São Paulo, SP, Brasil.

^cUniversidade de São Paulo, Escola Politécnica, Departamento de Engenharia Mecânica, Av. Prof. Mello Moraes, 2243, São Paulo, SP, Brasil.

^dUniversidade Presbiteriana Mackenzie, Rua da Consolação, 930, Consolação, São Paulo, SP, Brasil.

Received: December 13, 2022; Revised: April 06, 2023; Accepted: May 21, 2023

Ti alloys are widely used in severe corrosion environments where corrosion resistance is required, as biomedical industry. Additive manufacturing produces customized and complex products. Laser texturing is a process of structuring surfaces using laser pulses, that allows the creation of periodic patterns on the surfaces of materials, to modify them, functionally and/or aesthetically, in a precise and direct way, allowing parameterization, versatility and repeatability. Consequently, bringing together metallic additive manufacturing with laser texturing process could be an alternative to obtain parts with functional hydrophilic surfaces, which improves osteointegration and reduces bacteria adhesion. Thus, the aim of this work is to characterize and evaluate the influence of LASER parameters in as-built additive manufactured potential biomedical components. Ti6Al4V specimens were produced by L-PBF, using Ytterbium LASER with maximum power of 500 W, varying the laser power from 61 W to 244 W. The samples were characterized by SEM, Microhardness, and wettability. After that, some specimens were Laser textured using an Ytterbium optical fiber laser, and then evaluated by SEM, wettability, and 3D roughness. It was possible to observe that the surface of all studied samples was flattened after Laser texturing in comparison with as-built condition, due to the melting of the powder particles.

Keywords: LASER texturing, L-PBF, wettability.

1. Introduction

Titanium Ti6Al4V alloy (ISO5832-2) is the widely used titanium-based alloy in biomedical applications because of its unique properties, including higher corrosion resistance, elastic modulus like the bone and high mechanical strength to weight ratio in comparison with stainless steels and CoCrMo alloys¹. However, Ti6Al4V implants are traditionally produced by forging, casting and subtractive manufacturing, resulting in limited designs^{1,2}. Currently, most commercial orthopedic implants are machined, and their functional surface is made by ceramic coating, such as hydroxyapatite. However, these coatings generally detach, causing residual stress and cracks during the process, favoring corrosion of the metallic implant.

Additive manufacturing (AM) is a process of manufacturing 3D components, layer upon layer. It has been employed to build components with complex and customized lighter geometries³.

Various AM techniques have been developed and have different characteristics, but the Laser powder bed fusion (L-PBF) proved to be the most flexible process as is able to produce complex geometries components^{1,4,5}. This is due the printing information, that comes from a 3D model and it is executed layer by layer, using a laser with coordinated movements. Besides, this process can be applied in a large range of metallic alloys. The use of additive manufacturing to produce personalized implant reduces gaps between bone and implant, promoting faster patient healing. AM implants can also mix porous scaffolds and solid parts into one component, facilitating the osseointegration process².

Laser texturing has developed to focus on the surface properties changing, such as corrosion resistance and wettability⁶⁻⁹. This last property can substitute coatings and electrochemical processes, producing a large number of micro-cavities used to reduce bacteria adhesion, to promote osseointegration and to diminish the patient's recovery time and avoid the need for new surgeries caused by infections^{10,11}.

*e-mail: gleicy.limaxavier@gmail.com

Ti6Al4V ideal L-PBF additive manufacturing parameters can not be considered as well established, as they depend not only on the LASER type and power but also on the powder characteristics. Therefore, laser power, speed scan, melt-pool status and powder layer distribution on the build surface, should be considered in the additive manufacturing process. The aim of this work is to characterize and evaluate the influence of additive manufacturing and LASER texturing parameters in potential biomedical components.

2. Experimental

Ti6Al4V specimens were produced by Laser-Powder Bed Fusion (L-PBF) additive manufacturing with the scan speed of 100 mm/s and power from 61 W to 244 W using an Ytterbium LASER with maximum power of 500 W. The equipment used to produce these specimens is an OmniSint 160, from Omnitek.

Some L-PBF as-built specimens were grinded with silicon carbide paper up to #600, and then polished with diamond suspension up to 1 μm . After that, they were washed with isopropanol, and etched with Kroll solution for 15 minutes, at room temperature and microstructural analysis were performed using scanning electron microscope (SEM) – Hitachi TM3000. Others were Laser textured using an Ytterbium optical fiber laser, with a wavelength of 1064 nm (infrared), nominal power of 50 Watts, pulse duration of 150 ns, frequency of 2 kHz, focal length of 254 mm and theoretical diameter of the beam at order of 70 μm ¹². The Laser texturing was performed in a P1000U GF LASER texturing machine.

The microhardness of L-PBF samples before laser texture were measured using a hardener tester Stuers, Duramin AC40, with a diamond indenter at an axial load of 1 Kgf, for a dwell time of 15 s. There were 7 indentations, with 0.7 mm between them.

The wettability of L-PBF samples before and after Laser texturing was calculated using a drop shape analyzer Kruss by a sessile drop contact angle method. The roughness of these specimens was measured using a LASER confocal microscope Olympus LEXT OLS4100. The measured area was 6.25 mm², using a cutoff of 0.8 mm.

All equipment used in this study are located at SENAI Innovation Institute for Advanced Manufacturing and Microfabrication. All tests were performed at least 3 times – in different areas of the samples - to assure the reproducibility of the results.

3. Results and Discussion

Figure 1 presents the microstructure of L-PBF specimens typical of additive manufactured Ti6Al4V, according to X-ray diffraction presented in previous studies¹³ and to the literature: needles of acicular primary ($> 20 \text{ nm}$), secondary ($10 - 20 \text{ nm}$), ternary ($1 - 10 \text{ nm}$) and quartic ($< 1 \text{ nm}$) martensite α' ¹⁴⁻¹⁸ and some pores for lack of fusion. The types of martensite phases were produced by the constant deposition and melting in the L-PBF process. The intensity of the thermal cycle establishes the formation of the microstructures and the phase constitution. As the bulk energy density decreased, the rapid heat dissipation and aggravated thermal cyclic generated and therefore, the volume fraction of the ternary and quartic martensitic phase α' increased.

Figure 2 shows as-built L-PBF samples, with countless unmelted powder particles on their surface and some pores, typical of the additive manufacturing process¹⁹. After Laser texturing, the unmelted particles could not detect indicating that surface was flattened. On the other hand, pores are more apparent on the L-PBF samples built using higher LASER power due to the balling effect¹⁹. These results agree with X-ray tomography analysis, shown in Figure 3, where the sample built using 244 W showed the higher number of pores (0.17%) in comparison with the other conditions.

The average microhardness for L-PBF samples as-built is shown in Figure 4. As the LASER power increases, there is a slight decrease in microhardness values. However, this variation is very low, since for a LASER power of 61 W, the microhardness value is $354.0 \pm 9.9 \text{ HV}$, and for a LASER power of 244 W, the microhardness value is $342 \pm 1.77 \text{ HV}$.

Figure 5 shows the wettability results of L-PBF samples before and after the LASER texturing. All as-built samples were hydrophilic but after the Laser texturing, there is a decrease in the contact angle. These results suggest that the contact angle is proportional to the Laser power and can be explained by the combination of the micro and nanostructure.

The roughness of both surfaces was evaluated, and results are presented in Table 1, presenting not only both the 3D average roughness (S_a) and maximum peak to valley height of the profile (S_z) surface roughness parameters but also the skewness or asymmetry of the profile about the mean line (S_{sk}) and the “tailedness” of the profile about the mean line (S_{ku}), permitting a greater understanding of surface morphology. In Figure 6 it is presented the schematic drawing of the parameters S_a , S_z , S_{sk} and S_{ku} .

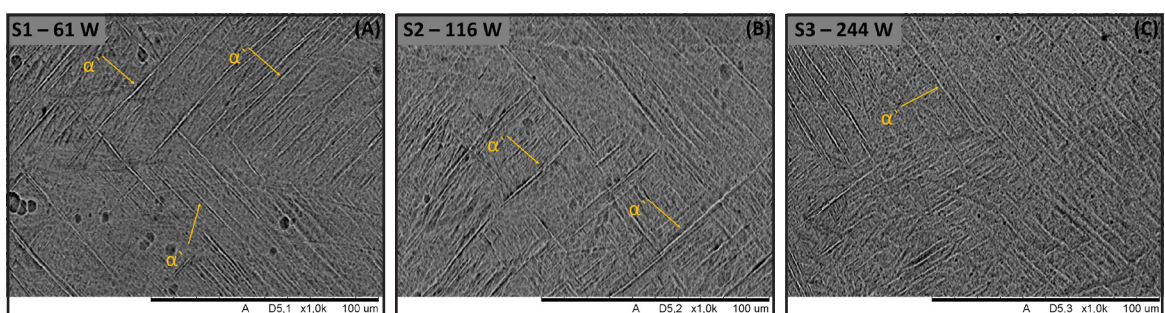


Figure 1. Micrographs of the L-PBF specimens presenting acicular martensite α' and some pores for lack of fusion. A) 61 W. b) 116 W and c) 244 W. Kroll reagent, 15 min, room temperature. SEM – BSE detector.

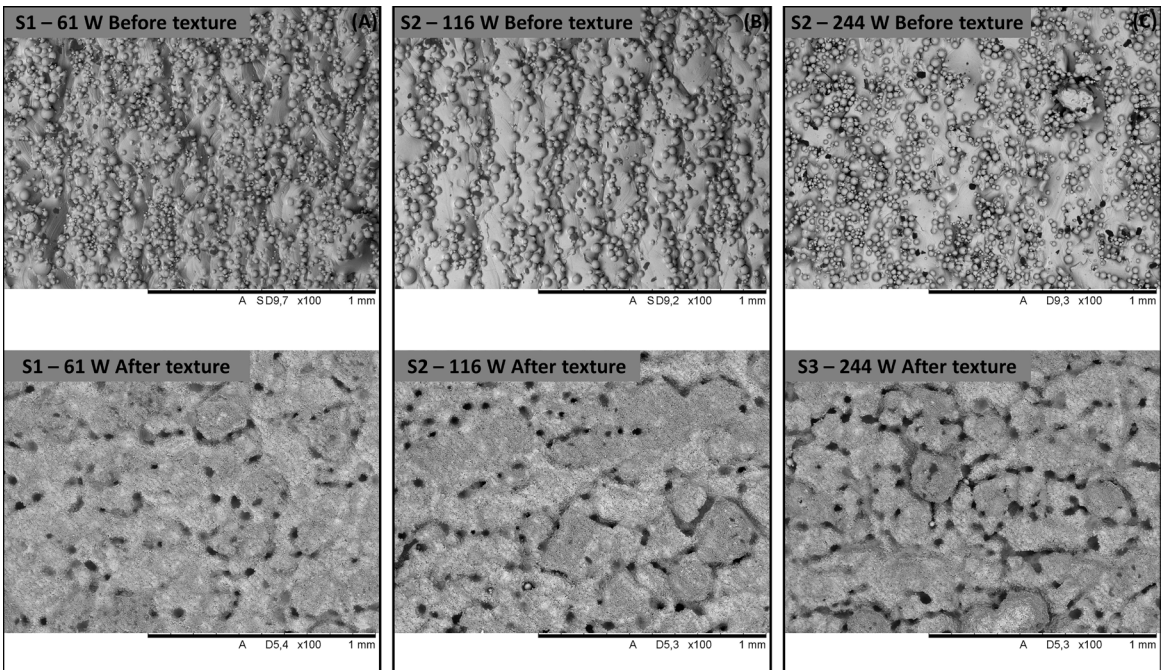


Figure 2. (A) Sample 1, built using 61 W, before and after texture; (B) Sample 2, built using 116 W, before and after texture; (C) Sample 1, built using 244 W, before and after texture.

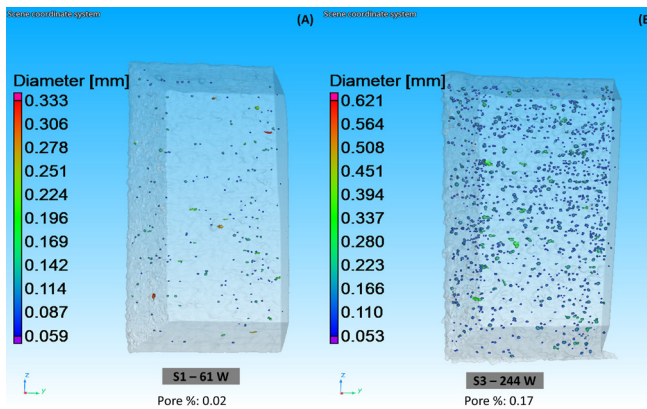


Figure 3. 3D porosity by x-ray tomography analysis. (a) Sample 1, built using 61 W; (b) Sample 2, built using 244 W.

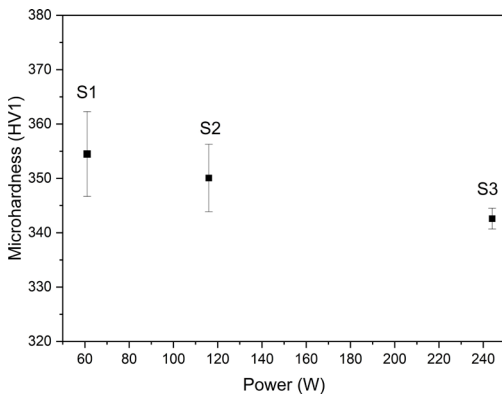


Figure 4. Microhardness values, obtained to Sample 1, 2 and 3, built using, respectively, 61 W, 116 W and 244 W.

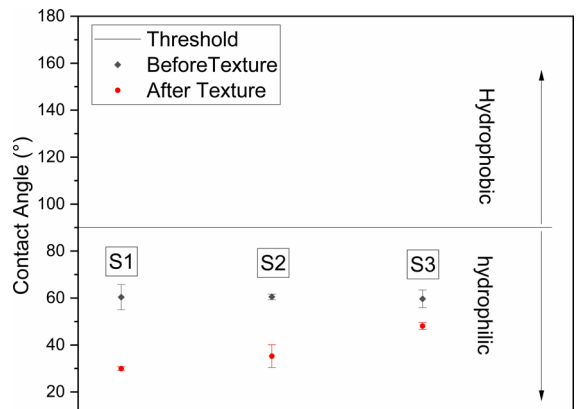


Figure 5. Wettability before and after laser texturing.

L-PBF and subsequent laser texturing process generated more homogeneous surfaces, with peaks and valleys arbitrarily distributed²⁰ – Figure 7, confirmed by the Sku topography parameter, remarkably close to 3. All Sz maximum values were one order of magnitude higher than their Sa, due to the texture on samples surfaces.

The Sku parameter showed that all Ti6Al4V samples presented a flat height distribution ($Sku < 4$)²¹. On the other hand, all samples presented negative Ssk, due to higher number of deep valleys in comparison with high peaks, confirming the decrease of partially melted powder particles on the surface.

Table 1. Roughness measurements of L-PBF Ti6Al4V after LASER texturing – Sa, Sz, Sku and Ssk parameters.

Sample	Sa (μm)	Sz (μm)	Sku (μm)	Ssk (μm)
AM 1 – 61 W	24.90 ± 2.32	164.84 ± 17.03	2.97 ± 0.18	-0.15 ± 0.25
AM 2 – 116 W	20.62 ± 2.61	142.25 ± 10.55	3.06 ± 0.5	-0.31 ± 0.11
AM 3 – 244 W	23.25 ± 4.86	156.07 ± 39.24	3.14 ± 0.38	-0.40 ± 0.14

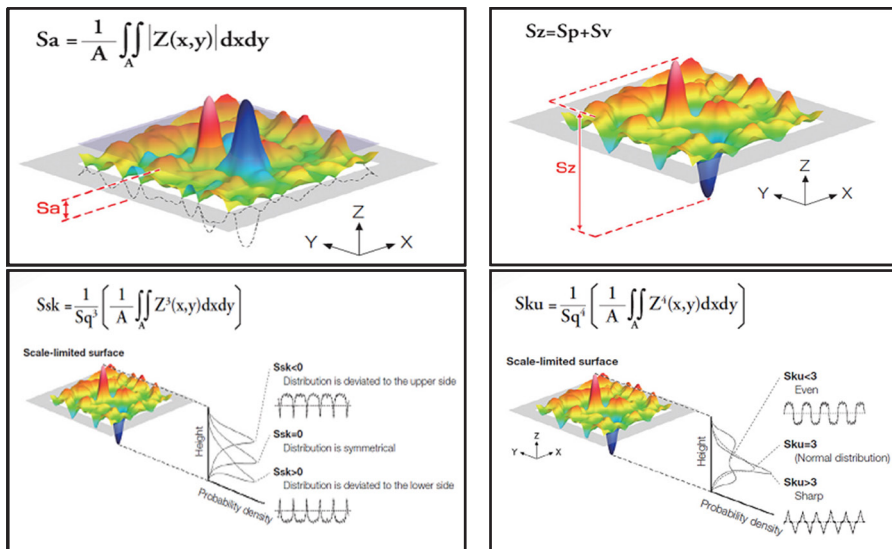


Figure 6. Schematic drawing about the parameters Sa, Sz, Ssk and Sku.²⁶

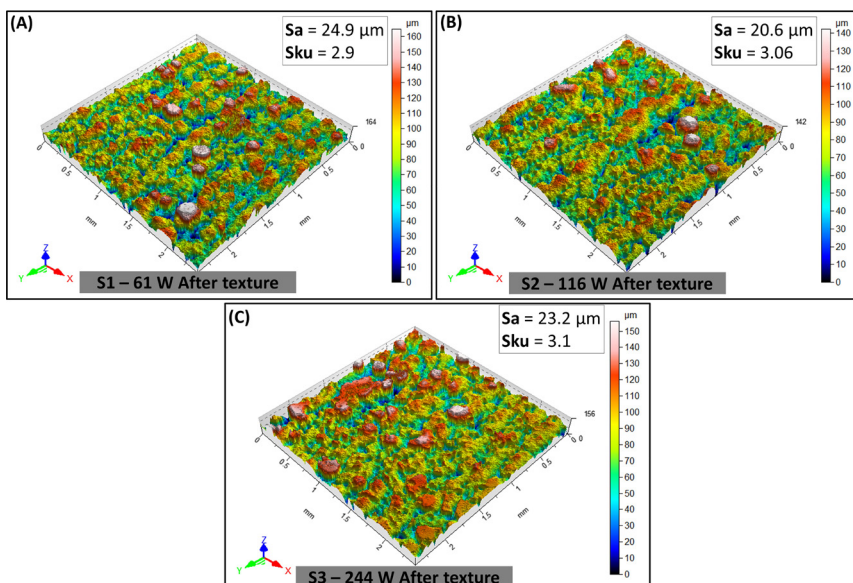


Figure 7. Roughness after laser texturing show peaks and valleys evenly distributed.

On the other hand, literature reports that bone-forming cells were more expected to attach to micro-nanostructure randomly distributed on surfaces than those with a higher degree of wettability²³⁻²⁴. Besides, tests with dermal cells suggests cell membrane adhere to shallow and large microgrooves (1 - 20 μm wide) but overpass deeper and narrower grooves (0.5 - 5.4 μm). This could explain why high roughness is not able to increase significantly the cell adhesion²⁵.

4. Conclusions

This study presents LASER texturing of L-PBF Ti6Al4V samples built at different LASER power. Their microstructure, microhardness, wettability and roughness were evaluated and compared.

The surface of all studied samples was flattened after Laser texturing in comparison with as-built condition, due to the melting of the powder particles. Besides, it was possible to obtain hydrophilic surfaces on all the samples, combining L-PBF with laser texturing. On the other hand, the lower roughness was obtained for the samples printed using medium Laser power.

The combination of microhardness, wettability and roughness results suggest that the sample built at medium Laser Power (116 W) presented the best characteristics to build components.

5. References

- Bartolomeu F, Gasik M, Silva FS, Miranda G. Mechanical properties of Ti6Al4V fabricated by laser powder bed fusion: a review focused on the processing and microstructural parameters influence on the final properties. *Metals*. 2022;12(6):986.
- Wong KC, Scheinemann P. Additive manufactured metallic implants for orthopaedic applications. *Sci China Mater*. 2018;61:440-54.
- García-León RA, Gómez-Camperos JA, Jaramillo HY. Scientometric review of trends on the mechanical properties of additive manufacturing and 3D printing. *J Mater Eng Perform*. 2021;30:4724.
- Geetha M, Singh AK, Asokamani R, Gogia AK. Ti based biomaterials, the ultimate choice for orthopaedic implants – a review. *Prog Mater Sci*. 2009;54(3):397-425.
- Wang K. The use of titanium for medical applications in the USA. *Mater Sci Eng A*. 1996;213(1-2):134-7.
- Ahuir-Torres JI, Arenas MA, Perrie W, Dearden G, Damborenea J. Surface texturing of aluminium alloy AA2024-T3 by picosecond laser: effect on wettability and corrosion properties. *Surf Coat Tech*. 2017;321:279-91.
- Cai Y, Luo X, Maclean M, Qin Y, Duxbury M, Ding F. A single-step fabrication approach for development of antimicrobial surfaces. *J Mater Process Technol*. 2019;271:249-60.
- He A, Liu W, Xue W, Yang H, Cao Y. Nanosecond laser ablated copper superhydrophobic surface with tunable ultrahigh adhesion and its renewability with low temperature annealing. *Appl Surf Sci*. 2018;434:120-5.
- Vilhena LM, Sedlaček M, Podgornik B, Vižintin J, Babnik A, Možina J. Surface texturing by pulsed Nd:YAG laser. *Tribol Int*. 2009;42(10):1496-504.
- Elias CN, Oshida Y, Lima JHC, Muller CA. Relationship between surface properties (roughness, wettability and morphology) of titanium and dental implant removal torque. *J Mech Behav Biomed Mater*. 2008;1(3):234-42.
- Cunha A, Elie A-M, Plawinski L, Serro AP, Rego AMB, Almeida A et al. Femtosecond laser surface texturing of titanium as a method to reduce the adhesion of *Staphylococcus aureus* and biofilm formation. *Appl Surf Sci*. 2016;360:485-93.
- Santos RG. Influência de parâmetros do laser pulsado de itérbio na modificação de superfícies da liga Ti-6Al-4V [dissertation]. São Paulo: Universidade de São Paulo; 2022.
- Oliveira RR, Ribeiro GX, Castro RS, Joaquim FB, Santos LU, Terada M et al. Caracterização de peças de Ti6Al4V produzidas por fusão em leito de pó e modificação superficial usando laser de nanosegundo. In: 24º Congresso Brasileiro de Engenharia e Ciência dos Materiais; 2022 Nov 6-10; Águas de Lindóia. Proceedings. São Carlos: DEMA/UFSCar; 2022.
- Yang J, Yu H, Yin J, Gao M, Wang Z, Zeng X. Formation and control of martensite in Ti-6Al-4V alloy produced by selective laser melting. *Mater Des*. 2016;108:308-18.
- Karimi J, Suryanarayana C, Okulov I, Prashanth KG. Selective laser melting of Ti6Al4V: effect of laser re-melting. *Mater Sci Eng A*. 2021;805:140558.
- Sun J, Zhu X, Qiu L, Wang F, Yang Y, Guo L. The microstructure transformation of selective laser melted Ti-6Al-4V alloy. *Mater Today Commun*. 2019;19:277-85.
- Lakroune Y, Connétable D, Hugues J, Hermantier P, Barriobero-Vila P, Dehmas M. Microstructural evolution during post heat treatment of the Ti-6Al-4V alloy manufactured by laser powder bed fusion. *J Mater Res Technol*. 2023;23:1980-94.
- Asherloo M, Wu Z, Sabisch JEC, Ghamarian I, Rollett AD, Mostafaei A. Variant selection in laser powder bed fusion of non-spherical Ti-6Al-4V powder. *J Mater Sci Technol*. 2023;147:56-67.
- Tolochko NK, Mozzharov SE, Yadroitsev IA, Laoui T, Froyen L, Titov VI et al. Balling processes during selective laser treatment of powders. *Rapid Prototyping J*. 2004;10(2):78-87.
- Anselme K, Bigerelle M, Nol B, Iost A, Hardouin P. Effect of grooved titanium substratum on human osteoblastic cell growth. *J Biomed Mater Res*. 2002;60(4):529-40.
- Aufa AN, Hassan MZ, Ismail Z, Harun N, Ren J, Sadali MF. Surface enhancement of Ti-6Al-4V fabricated by selective laser melting on bone-like apatite formation. *J Mater Res Technol*. 2022;19:4018-30.
- Aufa AN, Hassan MZ, Ismail Z. Recent advances in Ti-6Al-4V additively manufactured by selective laser melting for biomedical implants: prospect development. *J Alloys Compd*. 2022;896:163072.
- Aufa AN, Hassan MZ, Ismail Z. The fabrication of titanium alloy biomedical implants using additive manufacturing: a way forward. *J Miner Met Mater Eng*. 2021;7:39-48.
- Chesmel KD, Black J. Cellular responses to chemical and morphologic aspects of biomaterial surfaces. I. A novel in vitro model system. *J Biomed Mater Res*. 1995;29(9):1089-99.
- Walboomers XF, Monaghan W, Curtis ASG, Jansen JA. Attachment of fibroblasts on smooth and microgrooved polystyrene. *J Biomed Mater Res*. 1999;46(2):212-20.
- Evident [homepage on the Internet]. Tokio: Evident/Olympus; c2023 [cited 2023 Mar 29]. Available from: [https://www.olympus-ims.com/en/metrology/surface-roughness-measurement-portal/parameters/#!cms\[focus\]=areal-method](https://www.olympus-ims.com/en/metrology/surface-roughness-measurement-portal/parameters/#!cms[focus]=areal-method)